Ferromagnetic and Antiferromagnetic Exchange Coupling in bcc Epitaxial Ultrathin Fe(001)/Cu(001)/Fe(001) Trilayers

B. Heinrich, Z. Celinski, J. F. Cochran, W. B. Muir,[a] J. Rudd, Q. M. Zhong, A. S. Arrott, and K. Myrtle
Surface Physics Laboratory, Physics Department, Simon Fraser University, Burnaby, British Columbia, Canada V5A 1S6

J. Kirschner
Physics Department, Free University, Berlin 33, West Germany
(Received 12 October 1989)

We have grown a new phase of Cu, bcc Cu, on bcc Fe(001). We have shown that bcc Cu(001) grows epitaxially on bcc Fe(001) and that bcc Fe(001) grows epitaxially on bcc Cu(001). bcc Cu(001) on Fe(001) maintains its structure for 10–11 monolayers before undergoing a structural transition. Ultrathin well-defined trilayers of Fe(001)/Cu(001)/Fe(001) with Cu thicknesses between 6 and 12 monolayers were grown. Ferromagnetic resonance, Brillouin light scattering, and the surface magneto-optical Kerr effect were used to measure the coupling between the Fe layers. The coupling between the Fe layers changed from ferromagnetic to antiferromagnetic between 9 and 10 monolayers of Cu.

PACS numbers: 75.50.Bb, 75.70.Ak

Magnetic interactions between ferromagnetic films separated by nonmagnetic interlayers have attracted considerable interest.[1-3] The giant magnetoresistance observed in antiferromagnetically coupled Fe layers has raised expectations of exciting applications of these structures in the near future.[2] At the same time, metastable structures have been grown on (001) templates.[4-6] Unique magnetic properties are being engineered by growing metastable epitaxial overlayers of bcc Ni(001) on Fe(001) ultrathin substrates.[4] In fact, it was the structural modification that occurs in bcc Ni,[4,7] which resulted in a significant enhancement of the fourth-order in-plane anisotropy, that turned our attention to the growth of Cu on bcc Fe(001) substrates. Since Ni overlayers adopt the lattice structure of bcc Fe(001) in the early stages of their growth on Fe(001) substrates[8,9] it was reasonable to expect that Cu(001) overlayers would behave similarly and form a bcc metastable structure on a Fe(001) template.

As we show, bcc Cu(001) can be grown on Fe(001) and vice versa. This allows us to grow sandwiches of Fe(001) separated by various thicknesses of Cu and enables us to study the range of Fe spin-density penetration into nonmagnetic Cu. We also show that bcc Cu(001) grown on Fe(001) undergoes a structural modification with increasing thickness which is similar to the structural modification observed in Ni when it is grown on Fe(001). An understanding of the effects of the structural modification in the simpler nonmagnetic Cu case will help us to understand the role played by the Ni(001) structural modification in the enhanced magnetic anisotropies observed in Fe/Ni bilayers. This Letter reports on the exchange interaction between bcc Fe layers separated by bcc Cu. The exchange changes from ferromagnetic to antiferromagnetic at 9 ML (monolayers) of Cu and goes through an antiferromagnetic maximum near 12 ML. The magnetic properties were determined by ferromagnetic resonance (FMR), Brillouin light scattering (BLS), and the surface magneto-optical Kerr effect (SMOKE).

Fe(001)/Cu(001) and Cu(001)/Fe(001) bilayers and Fe(001)/Cu(001)/Fe(001) trilayers were grown by molecular-beam epitaxy on Ag(001) singular bulk substrates ($\theta < 0.25°$). Our previous experience shows that Ag(001) is an exceptionally good substrate for Fe(001) growth.[4,7,10] The epitaxial growth was carried out in the low-10^{-10} Torr range. The details of the Fe(001) growth and Ag(001) substrate preparation can be found in our previous paper.[4] The Cu was evaporated from a tantalum boat onto a Fe substrate maintained at 300 K.

Cu(001) overlayers grow layer by layer on Fe(001) substrates (see Fig. 1). They maintain the in-plane symmetry of the Fe(001) substrates for the first 10–11 ML. For comparison, Ni(001) overlayers can be grown that way for the first 3–6 ML. The reflection high-energy electron diffraction (RHEED) streak separations for Cu(001) overlayers are approximately 1.2% smaller than those for the Fe(001) layers indicating a corresponding increase in the Cu(001) in-plane lattice spacing. It would require a 12.5% distortion to match fcc Cu to bcc Fe. RHEED is generally not sensitive to the vertical lattice spacing. The anti-Bragg angle[11] for Fe growth on a Fe(001) whisker substrate was very close to the anti-Bragg condition for bcc Cu grown on Fe(001). That implies that the vertical interference conditions are very similar.[12] One can therefore argue that the Cu(001) overlayers grow in a nearly perfect bcc structure. Angular-resolved x-ray photoemission spectroscopy measurements[5] show that the vertical distortion of bcc Cu(001) grown on Ag(001) substrates is rather small. Ultimately vertical distortions and appropriate surface relaxations of bcc Cu(001) grown on Fe(001) will be

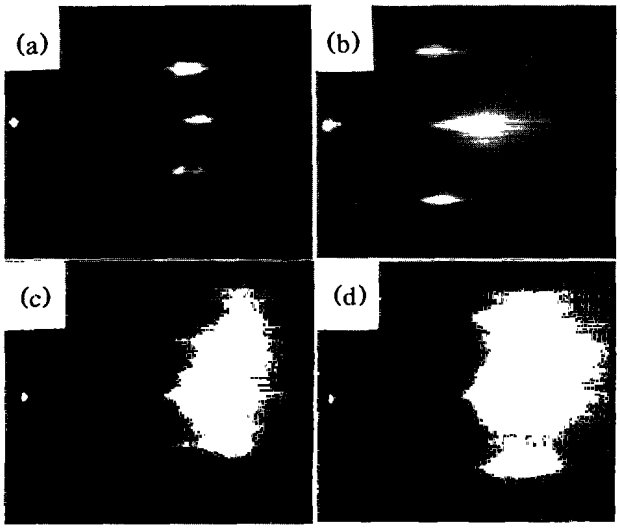

FIG. 1. RHEED patterns: (a),(b) in 6 ML Cu(001) grown on 5 ML bcc Fe(001); (c),(d) in 11.6-ML lattice-modified Cu(001) structure grown on 5 ML Fe(001). (a),(c) and (b),(d) show {10} and {11} azimuths, respectively.

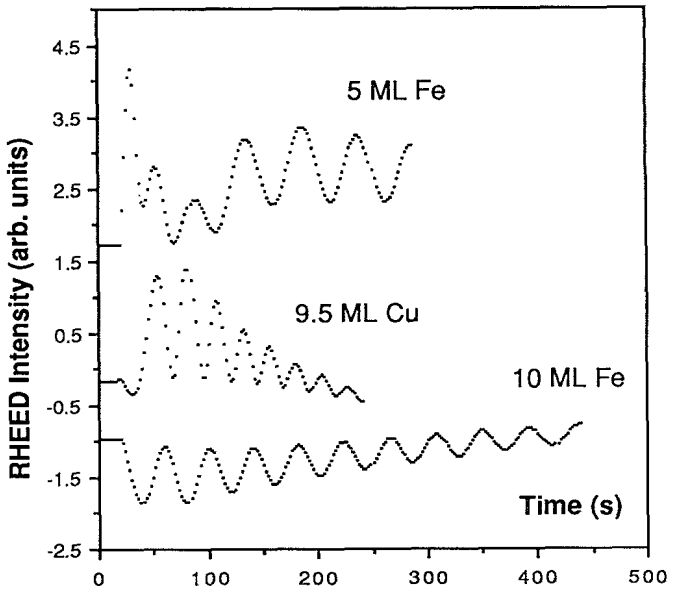

FIG. 2. RHEED intensity oscillations measured at the specular spot during the growth of the (5.0Fe/9.5Cu/10.0Fe) trilayer. 5 ML Fe(001) was grown on a Ag(001) substrate. The period of oscillations corresponds to the time required to form one atomic layer.

determined by LEED studies. In this Letter the term "bcc structure" will be used to characterize the growth of the first 10 ML of bcc Cu(001) on Fe(001) substrates without resolving the question of tetragonality.

The presence of large RHEED intensity oscillations during the growth of Cu(001) indicates that the Cu(001) layers were formed in a good layer-by-layer mode (see Fig. 2). RHEED patterns were significantly altered when the Cu(001) overlayers reached a critical thickness of 10 ML; see Fig. 1. The structural modification of bcc Cu(001) is different from that observed in the case of bcc Ni(001). The {10} azimuths developed two additional symmetrically spaced streaks (see Fig. 1), suggesting that the Cu(001) superlattice repeats along the {10} azimuths every three unit cells. The Cu {11} RHEED azimuths are, however, somewhat reminiscent of those for modified bcc Ni(001).[4] Superlattice streaks along the {11} azimuths do not seem to be commensurate with the lattice (see Fig. 1). This is similar to our observations on lattice-modified Ni(001) grown on Fe(001).[4] The Cu(001) superlattice streaks appeared close to the regular {11} bcc streaks (see Fig. 1), in contrast to the lattice-modified Ni(001) where they were located nearly centrally between the {11} streaks. The bcc Fe(001) overlayers grew in a good layer-by-layer mode even when deposited over lattice-modified Cu(001) films; see Fig. 2. All structures studied were epitaxially covered by 20 ML of Au(001) prior to their removal from UHV.

The theory of exchange-coupled ultrathin bilayers has been extensively reviewed in our recent papers.[4,13] In ultrathin films the magnetizations within individual layers are uniform. This condition converts our coupled Fe layers into the well-known model of exchange-coupled sublattices. There are two resonance modes: the low-frequency acoustic mode in which all magnetizations are parallel and the optical mode in which rf magnetizations oscillate out of phase. In our theoretical treatment,[4] the

TABLE I. Magnetic parameters of single and coupled Fe layers. The notation of (xFe/yCu/zFe) describes samples with x ML Fe grown on Ag(001) substrates, y ML Cu grown on x ML Fe, z ML Fe grown on y ML Cu, and covered by 20 ML Au(001). The magnetic parameters $(4\pi M_s)_{\text{eff}}$ and $2K_1/M_s$ were obtained from the FMR acoustic-mode peak measured at 36 GHz and assuming $g=2.09$ (Ref. 10). $(4\pi M_s)_{\text{eff}} = 4\pi M_s - H_s$, where H_s is the uniaxial anisotropy effective field perpendicular to the sample surface. $2K_1/M_s$ is the strength of the in-plane fourth-order anisotropy field (Ref. 4). A^{AB} was determined by fitting the FMR field of the optical mode and using magnetic parameters of the individually measured Fe layers (the first two entries in this table). To convert to surface energy multiply A^{AB} by $4/a = 1.4\times10^8$ cm^{-1}.

	$(4\pi M_s)_{\text{eff}}$ (kG)		$2K_1/M_s$ (kOe)		$10^9 A^{AB}$ (ergs/cm)	
Sample	295 K	77 K	295 K	77 K	295 K	77 K
9.0Cu/10.0Fe	13.53	13.75	0.259	0.286	···	···
5.0Fe/12.0Cu	3.08	1.72	0.113	0.283	···	···
5.0Fe/9.5Cu/10.0Fe	11.42	9.97	0.23	0.405	−1.32	···
5.0Fe/11.6Cu/10.3Fe	11.41	9.8	0.25	0.41	−1.6	···
4.8Fe/12.6Cu/9.0Fe	13.33	12.32	0.26	0.416	−1.0	−1.72
9.5Fe/8.7Cu/5.0Fe	7.98	6.32	0.30	0.33	>0[a]	···
5.0Fe/6.0Cu/11.0Fe	9.1	8.0	0.207	0.385	>0[a]	···

[a]Only acoustic mode visible.

exchange interface energy, E^{AB}, is given by

$$E^{AB}=4(A^{AB}/a)(\mathbf{M}^A/M^A)\cdot(\mathbf{M}^B/M^B),$$

where A^{AB} is the exchange-coupling coefficient between layers, M^A, M^B are the saturation magnetizations of layers A and B, respectively, and a is the lattice constant (assumed to be the same in both layers).

Our experimental results were analyzed numerically using a theory which includes a full treatment of demagnetizing fields and magnetic surface and bulk anisotropies.[4] The results of this analysis are summarized in Table I. The most important results are shown in the first three rows. Rows 1 and 2 show measured magnetic properties of the individual Fe layers. Using these properties and a single interaction parameter, A^{AB}, we can account very well for both the acoustical and optical peaks in the FMR resonance spectrum of the trilayer in row 3. The fit is shown in Fig. 3 where it is seen that the resonance intensities of the acoustic and optical modes scale precisely according to theory. We would like to point out that this theory predicts that the optical-mode intensity is absent in ultrathin structures having identical ferromagnetic layers.[4] In our case we used different thicknesses which resulted in different perpendicular uniaxial anisotropies and hence different resonance frequencies. All trilayers with Cu interlayer thicknesses d larger than 9 ML exhibit two resonance peaks in FMR and BLS measurements. The weaker peaks, corresponding to the optical modes, were always located at higher fields (FMR) and lower frequencies (BLS) than the FMR fields and BLS frequencies of acoustic modes; see Figs. 3 and 4. This shows unambiguously that the Fe(001) layers were coupled antiferromagnetically. In the thicker samples the Cu had undergone a structural modification of the bcc lattice, but the sample with $d_{Cu}=9.5$ ML remained unmodified. The existence of antiferromagnetic coupling does not depend upon the change in structure. The observed values of the coupling parameter are consistent with a maximum between 11 and 12 ML for antiparallel coupling through Cu.

Trilayers having bcc Cu(001) interlayers thinner than 9 ML coupled the Fe layers so strongly that only the acoustic modes were observed. The individual layer magnetizations were found to be parallel at 8.5 kOe as determined from the total trilayer magnetic moment measured by means of the FMR intensity.[7] BLS measurements, carried out over the dc magnetic field range $0<H<8$ kOe, did not show any change in the static

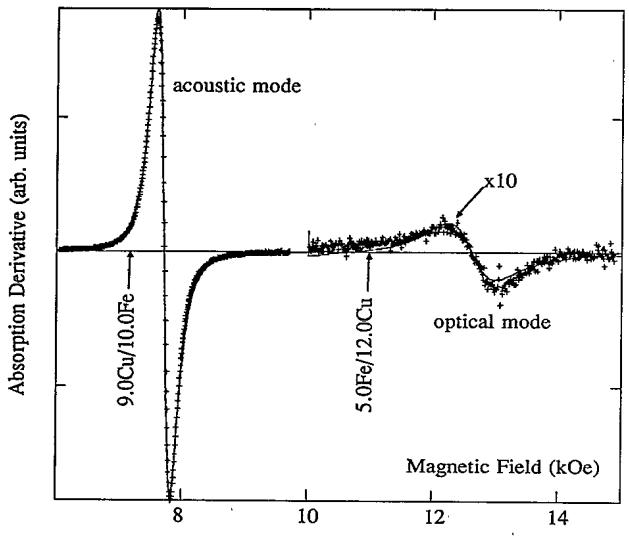

FIG. 3. Field derivative of FMR absorption in the (5.0Fe/9.5Cu/10.0Fe) trilayer (+). The solid line was calculated using the theory of exchange-coupled Fe layers. The only fitting parameter was the strength of exchange coupling, $A^{AB}=1.3\times10^{-9}$ erg/cm. The magnetic parameters of the individual Fe layers were determined in separate measurements; see the first two entries in Table I. The strength of the optical mode is significantly weaker than the strength of the acoustic mode due to both the increased stiffness of the optical mode ($\sim 8\times$) and an appreciable increase in the optical resonance linewidth. The arrows indicate the FMR fields expected for the individual Fe layers.

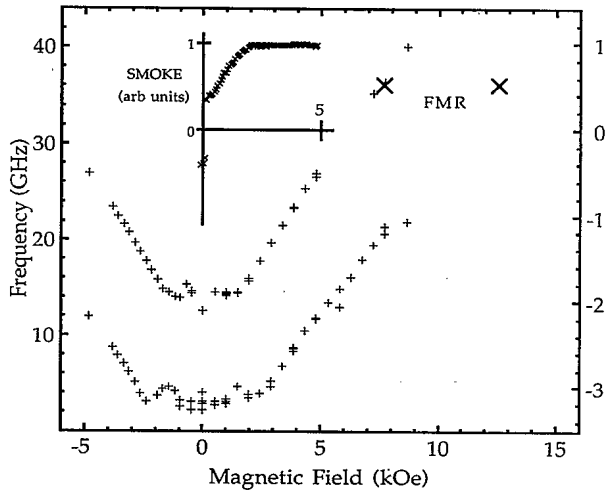

FIG. 4. Magnetic excitation frequencies vs external magnetic field, H, measured by means of BLS for the trilayer specimen (5.0Fe/11.6Cu/10.3Fe). For $|H|>2$ kOe the magnetizations in the two Fe films become parallel; in this case the high-frequency mode corresponds to the acoustic mode and the low-frequency mode corresponds to the optical mode. The ratio of intensities, acoustic/optical ~ 3 for fields greater than 3 kOe, is in agreement with a calculation (Ref. 13) based upon negative exchange coupling. The low-field structure is reproducible. Inset: The SMOKE rotation in the (5.0Fe/9.5Cu/10.0Fe) trilayer with the magnetic field along the magnetic easy axis (100). For $H<2$ kOe, Fe magnetizations rotate away from the applied field. For $H<500$ Oe the moments in the two layers are opposed, reducing the magnetization by nearly $\frac{1}{3}$ as expected. For $H<40$ Oe, the magnetization reverses direction.

magnetic configuration. BLS and FMR spectra were described quite adequately by field-independent magnetic parameters. Therefore the Fe(001) layers separated by bcc Cu(001) interlayers less than 9 ML thick are coupled ferromagnetically; that is, $A^{AB} > 0$.

The FMR and BLS results show that the coupling between Fe layers changes from ferromagnetic to antiferromagnetic when the Cu(001) interlayer thickness reaches ~9 ML. The strength of the antiferromagnetic coupling, A^{AB}, predicts the value of the applied dc field, H_p, at which the collinearity condition between the layer magnetizations is not satisfied. A minimization of the interface, Zeeman energies, and anisotropy energies (with dc field along the easy magnetic axis) results in

$$H_p + 2K_1/M_s = (4A^{AB}/aM_s)(1/d_A + 1/d_B).$$

Using A^{AB} and $2K_1/M_s$ parameters for the (5.0Fe/9.5Cu/10.0Fe) trilayer from our resonance measurements (see Table I) leads to $H_p = 2.0$ kOe. SMOKE showed indeed (see Fig. 4, inset) that for dc applied fields less than 2 kOe the Fe magnetizations started to rotate away from the dc applied field. There is a range of low fields less than 500 Oe over which the moments in the two layers are opposed, reducing the magnetization almost by a factor of 3. For a field which is less than 40 Oe the magnetization suddenly reverses its direction by domain-wall nucleation and subsequent propagation; see the negative SMOKE signal in the inset of Fig. 4. The loss of collinearity is also evident in the BLS measurements from an obvious nonmonotonic dependence of BLS resonant frequencies on dc field for fields less than 2 kOe.

It is important to point out that the reconstructed Cu(001) overlayers did not enhance the fourth-order in-plane anisotropy in Fe: Crystallographic defects created during the lattice reconstruction are not sufficient on their own to introduce large in-plane anisotropies. Therefore for Fe/Ni bilayers the large increases in the fourth-order in-plane anisotropy observed for the lattice-transformed Fe/Ni(001) bilayers[4] were a consequence of an additional magnetic energy created by the broken symmetry around the network of symmetrically distributed crystallographic defects in the Ni.

In conclusion, (1) metastable phases of epitaxial bcc Cu(001) overlayers were grown on Fe(001) and identified by RHEED patterns. (2) The Cu(001) lattice transformation in Fe/Cu(001) bilayers does not lead to increased in-plane anisotropies as was observed in lattice-modified Fe/Ni(001) bilayers. (3) The magnetic coupling in Fe/Cu/Fe trilayers changes from ferromagnetic to antiferromagnetic when the Cu(001) interlayer thickness reaches ~9 ML. The Cu(001) layer thickness at the crossover to antiferromagnetic coupling is larger than observed for Cr(001), $d_{Cr} = 6$ ML.[2,3,14] We note that Cu unlike Cr has no holes in its d band. That presents a challenge to theorists. (4) dc applied fields, required to switch from the antiparallel to the parallel configuration, are significantly lower for Fe/Cu/Fe trilayers than for $[Fe/Cr/Fe]_n$ superlattices exhibiting a giant magnetoresistance. Therefore the Fe/Cu/Fe(001) structures are an attractive candidate for the study of the magnetoresistance in antiferromagnetically coupled superlattices.

The authors would like to thank the National Research Council of Canada for financial support and K.B. Urquhart for his help in preparing some of the drawings.

[a]Permanent address: Physics Department, McGill University, Montreal, Quebec, Canada H3A 2T8.

[1]F. Saurenbach, V. Waltz, L. Hinchey, P. Grunberg, and W. Zinn, J. Appl. Phys. **63**, 3473 (1988).

[2]M. N. Baibich, J. M. Broto, A. Fert, F. Nguyen Van Dan, E. Petroff, P. Etienne, G. Creuzet, A. Friedrich, and J. Chazelas, Phys. Rev. Lett. **61**, 2472 (1988).

[3]J. J. Krebs, P. Lubitz, A. Chaiken, and G. A. Prinz, Phys. Rev. Lett. **63**, 1645 (1989).

[4]B. Heinrich, S. T. Purcell, J. R. Dutcher, K. B. Urquhart, J. F. Cochran, and A. S. Arrott, Phys. Rev. B **38**, 12879 (1988).

[5]W. F. Egelhoff, Jr., and I. Jacob, Phys. Rev. Lett. **62**, 921 (1988).

[6]C. M. Schneider, J. J. de Miguel, P. Bressler, J. Garbe, S. Ferrer, R. Miranda, and J. Kirschner, J. Phys. (Paris), Colloq. **49**, C8-1657 (1988).

[7]B. Heinrich, A. S. Arrott, J. F. Cochran, K. B. Urquhart, K. Myrtle, Z. Celinski, and Q. M. Zhong, Mater. Res. Symp. Proc. **151**, 177 (1989).

[8]B. Heinrich, A. S. Arrott, J. F. Cochran, C. Liu, and K. Myrtle, J. Vac. Sci. Technol. A **4**, 1376 (1986).

[9]Z. Q. Wang, Y. S. Li, F. Jona, and P. M. Marcus, Solid State Commun. **61**, 623 (1987).

[10]B. Heinrich, K. B. Urquhart, A. S. Arrott, J. F. Cochran, K. Myrtle, and S. T. Purcell, Phys. Rev. Lett. **59**, 1756 (1987).

[11]At the anti-Bragg angle the reflected beams from adjacent atomic planes are out of phase; therefore the minimum intensity observed during RHEED oscillations is very close to zero.

[12]A. S. Arrott, B. Heinrich, and S. T. Purcell, in "Kinetics of Ordering and Growth at Surfaces," edited by M. G. Lagally (Plenum, New York, to be published).

[13]J. F. Cochran and J. R. Dutcher, J. Appl. Phys. **64**, 6092 (1988).

[14]J. Barnas and P. Grunberg, J. Magn. Magn. Mater. (to be published).